## Title

Characterization of a diffuse intrinsic pontine glioma cell line: implications for future investigations and treatment.



## Journal

Journal of neuro-oncology, 110(3)

## ISSN

0167-594X

## Authors

Hashizume, Rintaro
Smirnov, Ivan
Liu, Sharon
et al.

## Publication Date

2012-12-01

## DOI

10.1007/s11060-012-0973-6

Peer reviewed

# *Characterization of a diffuse intrinsic pontine glioma cell line: implications for future investigations and treatment*

**Rintaro Hashizume, Ivan Smirnov, Sharon Liu, Joanna J. Phillips, Jeanette Hyer, Tracy R. McKnight, Michael Wendland, Michael Prados, et al**

**Journal of Neuro-Oncology**

ISSN 0167-594X

J Neurooncol
DOI 10.1007/s11060-012-0973-6

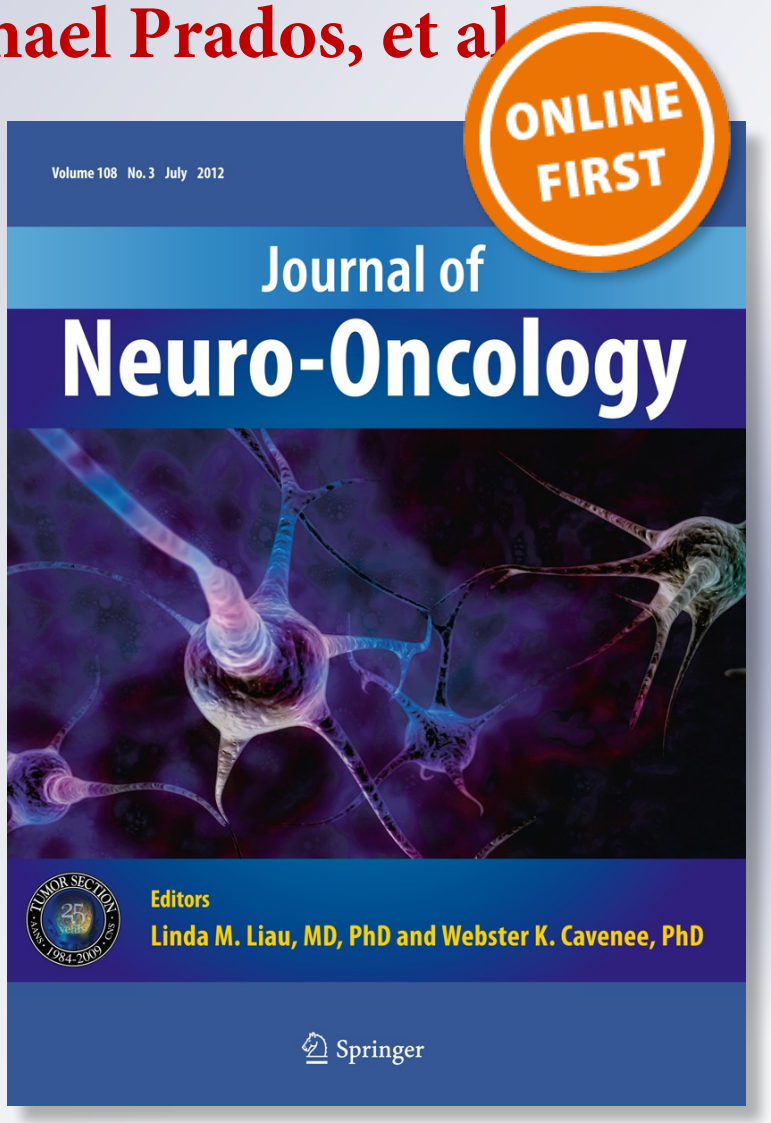


Springer

J Neurooncol
DOI 10.1007/s11060-012-0973-6

LABORATORY INVESTIGATION

# Characterization of a diffuse intrinsic pontine glioma cell line: implications for future investigations and treatment

**Rintaro Hashizume · Ivan Smirnov · Sharon Liu · Joanna J. Phillips · Jeanette Hyer · Tracy R. McKnight · Michael Wendland · Michael Prados · Anu Banerjee · Theodore Nicolaides · Sabine Mueller · Charles D. James · Nalin Gupta**

Received: 2 May 2012 / Accepted: 11 September 2012


**Abstract** Diffuse intrinsic pontine gliomas arise almost exclusively in children, and despite advances in treatment, the majority of patients die within 2 years after initial diagnosis. Because of their infiltrative nature and anatomic location in an eloquent area of the brain, most pontine gliomas are treated without a surgical biopsy. The corresponding lack of tissue samples has resulted in a limited understanding of the underlying genetic and molecular biologic abnormalities associated with pontine gliomas, and is a substantial obstacle for the preclinical testing of targeted therapeutic agents for these tumors. We have established a human glioma cell line that originated from surgical biopsy performed on a patient with a pontine glioma. To insure sustainable in vitro propagation, tumor cells were modified with hTERT (human telomerase ribonucleoprotein reverse transcriptase), and with a luciferase reporter to enable non-invasive bioluminescence imaging. The hTERT modified cells are tumorigenic in athymic rodents, and produce brainstem tumors that recapitulate the infiltrative growth of brainstem gliomas in patients.

**Keywords** Brainstem glioma · Animal model · Astrocytoma

R. Hashizume · I. Smirnov · S. Liu · J. J. Phillips · J. Hyer · T. R. McKnight · M. Prados · A. Banerjee · T. Nicolaides · S. Mueller · C. D. James
Department of Neurological Surgery, Brain Tumor Research Center, University of California San Francisco, San Francisco, CA 94143-0520, USA

J. J. Phillips
Department of Pathology, University of California San Francisco, San Francisco, CA 94143, USA

T. R. McKnight · M. Wendland
Department of Radiology and Biomedical Imaging, University of California San Francisco, San Francisco, CA 94143-0946, USA

A. Banerjee · T. Nicolaides · S. Mueller · N. Gupta
Department of Pediatrics, University of California San Francisco, San Francisco, CA 94143, USA

S. Mueller
Department of Neurology, University of California San Francisco, San Francisco, CA 94143, USA

N. Gupta (✉)
Department of Neurological Surgery, Brain Tumor Research Center, University of California San Francisco, 505 Parnassus Avenue, Room M779, San Francisco, CA94143-0112, USA
e-mail: guptan@neurosurg.ucsf.edu

## Introduction

Brainstem gliomas represent 10–15 % of brain tumors in children and show varying degrees of malignancy. The majority of brainstem gliomas, however, arise in the ventral pons in children less than 10 years of age, and are malignant neoplasms. The prognosis for patients with diffuse intrinsic pontine gliomas (DIPG) is very poor with very few individuals surviving more than 2 years after initial diagnosis [1, 2]. The factors that contribute to the dismal prognosis include extensive infiltration at the time of diagnosis, an eloquent anatomic location which precludes surgical resection, and resistance to most types of conventional cancer therapeutics that have been tested in clinical trials to date [2, 3]. Phase I studies conducted over the past 20 years have failed to demonstrate any meaningful improvement in survival for these patients [4].

A fundamental limitation in the development of biologically targeted therapies for DIPG is that the diagnosis is usually confirmed by imaging studies and surgical biopsy is

Published online: 17 September 2012

rarely performed. As a result, viable cell and/or tissue resources, for preclinical testing of therapeutic hypotheses, are very limited. Moreover, and in contrast to the enormous strides have been made in the understanding of the genetics of adult malignant glioma [5, 6], the lack of DIPG tissue samples has hindered progress in identifying underlying oncogenic steps that contribute to the development of DIPG. Recently, genetic analyses of tissues obtained at autopsy have identified a number of DIPG gene and chromosomal alterations, including mutation of the gene encoding histone H3, which is rare among adult malignant gliomas [7, 8]. These recent results support the existence of key genetic differences between adult gliomas and DIPGs, thereby underscoring the need for thorough molecular profiling of the brainstem tumors, for facilitating improved understanding of associated molecular biology, and the related development of rational therapeutic approaches for treating DIPG.

We have recently reported the development of an orthotopic animal model of a brainstem glioma in which tumor growth and therapeutic response can be accurately monitored by bioluminescence imaging (BLI) for preclinical therapeutic testing. Although this model recapitulates some of the anatomic features of the human disease, the cell source used was derived from an adult glioblastoma [9, 10]. Others have also relied on adult GBM as a cell source for modeling DIPG [11].

In this report, we describe the establishment of a primary DIPG cell line obtained from surgical biopsy performed on a 6 year old female patient, the utilization of these cells to model DIPG in athymic rats, with resultant tumors that recapitulate most of the features of the human disease. Gene expression and copy number analysis was also performed allowing comparison with previously reported cohorts of pediatric gliomas. This new cell resource should facilitate the testing of specific targeted therapeutics for brainstem glioma and promote personalized treatment strategies for the patients with this cancer. Isolation of a DIPG cell line has been described from autopsy-derived tissue [12]. Our report extends this work by demonstrating the feasibility of creating a human-derived DIPG tumor model obtained through a limited surgical biopsy prior to therapeutic intervention.

## Materials and methods

### Clinical history

A 6 year old girl presented with ataxia and diplopia over 2–3 weeks duration. An MRI scan of the brain demonstrated a non-enhancing infiltrative lesion centered in the ventral pons (Fig. 1). Using a frameless stereotactic system, two tissue specimens measuring approximately 1 × 3 mm in size were obtained through a trans-cerebellar route [13]. No complications were noted in the post-operative period related to the surgical procedure. The patient was treated with external beam radiotherapy (55 Gy), and capecitabine administered through participation in a Pediatric Brain Tumor Consortium clinical trial. The patient's symptoms worsened over several weeks and she died 7 months after diagnosis from progressive disease. Tumor tissue was acquired by the UCSF Tissue Bank through an approved Committee on Human Research protocol and assigned a unique identifier (SF7761). Informed consent was obtained from the subject's parents.

### Primary cell culture and modification of tumor cells

The biopsy tissue was minced with a scalpel and incubated in Papain solution (Worthington, NJ) at 37 °C for 20 min with shaking every few minutes to dissociate the tissue. The tissue was triturated using a sterile pipette until no clumps were visible, with the tissue suspension passed through a series of nylon mesh filters of 0.45–0.7 μm pore diameter. After centrifugation of the suspension, the cell pellets were washed with PBS and maintained as a neurosphere culture, as previously described [14].

The diagnostic histopathology of the tissue obtained from the surgical biopsy was consistent with an infiltrative astrocytoma, WHO grade II. Based on previous experience with establishing primary cell cultures from low grade glial tumors, we anticipated this tissue would have a low likelihood of engraftment, and would likely become senescent from extended cell culture. Therefore, we transduced SF7761 cells with a retrovirus vector containing human telomerase reverse transcriptase (hTERT) for cell immortalization after the second passage. Cells that were not immortalized underwent senescence over 1–2 weeks. Retroviral vectors were generated by transient transfection of 293T (human embryonal kidney) cells with plasmids encoding the vesicular stomatitis virus G envelope, gag-pol, and hTERT genes. Viral vectors were harvested from supernatant at 48 h after transfection, filtered (0.45 μm), and then used to infect the primary brainstem tumor cells. The immortalized tumor cells were subsequently transduced with a lentiviral vector containing firefly luciferase (Fluc), as previously described [15].

### Animals and surgical procedures

Six-week-old male athymic rats (rnu/rnu, homozygous) were purchased from the National Cancer Institute (Frederick, MD). Rats were housed in a temperature-controlled and light-controlled environment with an alternating 12-hour light/dark

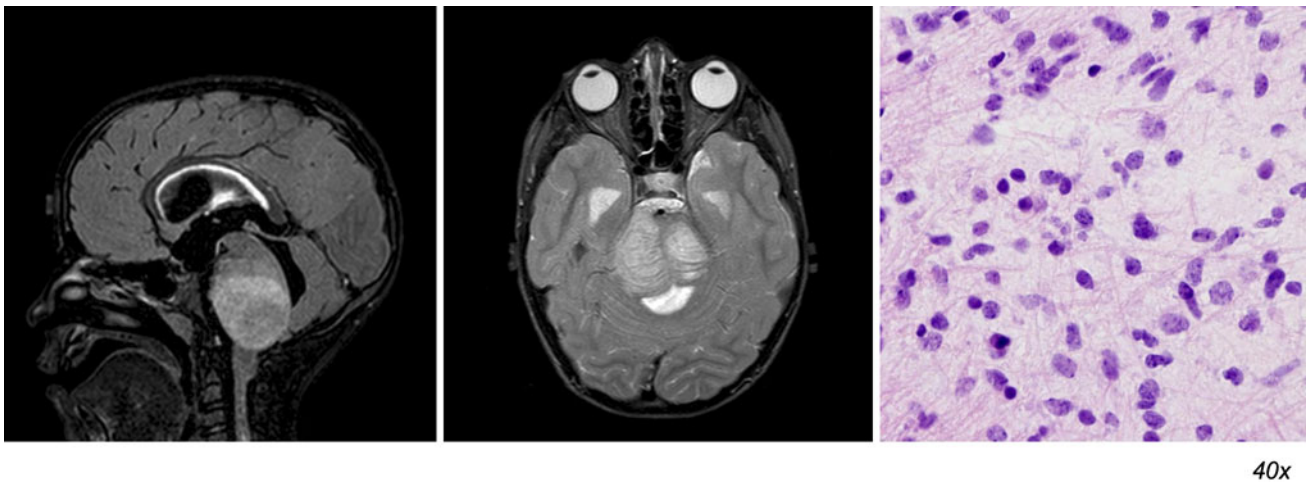


**Fig. 1** Imaging and pathologic features. Sagittal FLAIR (*left*) and axial T2-weighted (*middle*) images demonstrate a diffusely expanded pons consistent with a DIGP. No areas of heterogeneity were noted. A biopsy was performed from the right side of the pons through a transcerebellar route. The pathology (*right*) is consistent with an infiltrating astrocytoma

cycle. All protocols were approved by the UCSF Institutional Animal Care and Use Committee (IACUC).

Luciferase and hTERT modified primary brainstem tumor cells were injected into the pontine tegmentum of athymic rats using an implantable guide-screw system as described previously [9, 10]. Briefly, rats were anesthetized by intraperitoneal injection of 100 mg/kg of ketamine and 10 mg/kg of xylazine and positioned in a stereotactic device (David Kopf Instruments, Tujunga, CA) using ear bars. A burr hole was drilled through the skull 2.0 mm to the right of the midline, 9.6 mm behind the bregma, and 9.6 mm deep from the bottom of the skull. $1 \times 10^5$ tumor cells suspended in 1 μl HBSS were injected slowly (over 1 min) into the pontine tegmentum through the guide-screw. All procedures were carried out under sterile conditions.

## In vivo BLI monitoring

To monitor brainstem tumor growth in vivo, BLI was performed with the Xenogen IVIS Lumina System using LivingImage software for data acquisition (Xenogen Corp.). Rats were anesthetized with 100 mg/kg of ketamine and 10 mg/kg of xylazine and imaged 12 min after intraperitoneal injection of luciferin (D-luciferin potassium salt, 150 mg/kg, Gold Biotechnology, St Louis, MO). Signal intensity was quantified within a region of interest over the skull, as defined by the LivingImage software.

## MR imaging

All scans were performed on a Varian 7 Tesla small animal MR scanner with a 31 cm diameter horizontal bore. Animals were anesthetized with isofluorane and placed supine in an animal tray lined with a heating pad and equipped with an anesthesia mask to allow continuous breathing of a 1.5–2.5 % oxygen/isofluorane mixture. A bite bar affixed to the anesthesia mask served to immobilize the animal's head during the scans. A catheter was placed in the tail vein for subsequent injection of gadolinium contrast agent (Magnevist, Bayer Schering Pharma AG, Germany), a rectal probe was inserted to monitor the core body temperature, and lubricant was placed on the animals' eyes to prevent orbital dehydration. The animal and tray were then placed in the magnet, and a dose of 0.5 mmol/kg Magnevist was injected into the tail vein catheter. The following imaging sequences were then applied: (1) a series of eight sequential coronal T1-weighted spin echo image volumes (matrix = 128 × 128, slices = 12, field of view (FOV) = 40 mm × 40 mm, pixel size = 0.098 $mm^2$, slice thickness = 1 mm, TR = 550 ms, TE = 20 ms) to visualize the leakage of gadolinium across the blood-tumor barrier; and (2) two T2-weighted spin echo images acquired in the sagittal and coronal planes (matrix = 256 × 256, slices = 12 for coronal and 16 for sagittal, FOV = 40 mm × 40 mm, pixel size = 0.098 $mm^2$, slice thickness = 1 mm, TR = 3,000 ms, TE = 80 ms for coronal and 50 ms for sagittal) to delineate the tumor.

## Western blotting

Total cell lysate was collected from asynchronously proliferating cells in buffer (Cell Signaling) supplemented with proteinase (Roche) and phosphatase (Sigma) inhibitor cocktails. Lysates were resolved by SDS-PAGE, and transferred to polyvinylidene difluoride membranes. After probing with primary antibodies, the membranes were incubated with horseradish peroxidase-conjugated secondary antibody, and visualized by ECL (GE Healthcare).

Antibodies specific for PDGFRα (Upstate Biotechnology), EGFR (Santa Cruz Biotechnology), SNF5 (abcam), RB (4H1, Cell Signaling Technologies), p16 (BD Pharmingen), and β-actin (Ambion) were used.

### Gene expression and copy number analysis

RNA extraction from the cell line grown in vitro was performed using a standard protocol using the Ambion MirVana RNA isolation kit. Gene expression analysis was performed using Agilent 4 × 44 arrays (Sandler Center, UCSF). DNA from SF7761 cells was isolated according to a standard protocol (Affymetrix, Inc.). Microarray analysis using Affymetrix Genome-Wide Human SNP Array 6.0 was performed at the UCSF Genomics Core. A reference DNA sample provided by Affymetrix was used as a control.

Estimation of full-resolution copy number from the raw data was performed using Affymetrix Power Tools (APT) software package v. 1.14.3 [http://www.affymetrix.com/partners_programs/programs/developer/tools/powertools.affx], and PennCNV copy number variation detection tool v. 2011Jun16 [16]. Since PennCNV requires a large number of samples for reliable CNV calling, we added 2,234 blood samples data downloaded from The Cancer Genome Atlas (TCGA) data portal. Those 2,234 samples were selected from 3,416 samples by filtering out lower quality samples with Contrast QC <0.4, failed chrX/Y copy number probes ratio gender call and per sample genotype call rate <95 %.

## Results

### Establishment of a primary cell line

The initial disaggregated surgical specimen demonstrated decreasing growth in defined neurosphere media, and as a result a culture specimen was subjected to retroviral hTERT modification to insure sustainable propagation of the tumor cells. Non-transduced cells eventually became senescent. The hTERT modified cells displayed robust growth in culture, and to an extent allowing a sufficient number to be isolated for brainstem injection in rats. The doubling time of the hTERT modified cells in log phase growth was 48 h.

### Progressive growth of brainstem tumors measured by BLI

Injection of luciferase–hTERT modified human brainstem tumor cells ($1 \times 10^5$ cells in 1 μl HBSS) into athymic rats resulted in 100 % tumor take. BLI revealed readily detectable, quantifiable, and increasing signal from the tumors (Fig. 2a), supporting progressive tumor growth subsequent to tumor cell injection. All animals ultimately displayed typical posterior fossa symptoms, such as torticollis and nystagmus. Survival of rats, as determined by criteria necessitating euthanasia, ranged from 183 to 213 days after implantation. MRI imaging of rats was performed at 156 days after implantation. MRI did not show a discrete tumor mass, but rather a non-specific T2-signal abnormality in the rat pons (Fig. 2b). Gross examination of brains resected immediately following euthanasia did not show visible tumor either on the surface of the pons, nor after sectioning.

### Comparison of human brainstem glioma and brainstem tumor xenografts

Histopathologic analysis of the surgical biopsy revealed a typical infiltrating astrocytoma with neoplastic cells disseminated within a background of neural tissue. The histopathology of the tissue available for diagnostic purpose displayed features consistent with a WHO grade II astrocytoma (Fig. 1). Examination of corresponding xenografts in rat brainstems demonstrated a diffusely infiltrating tumor, similar to that observed in the surgical biopsy specimen (Fig. 2b). Xenograft tumor cells appeared to extend through the pons, and in some cases to expand the structure, also similar to that observed in patients with DIPG (Fig. 2c). Immunohistochemistry revealed that the infiltrating tumor in the pons was positive for GFAP, Nestin, Olig2, and PDGFRα (Fig. 2d).

### Protein and gene expression

Western blotting showed expression of PDGFRα, EGFR (wild type), Rb (endogenous total Rb) proteins, but lack of expression of $p16^{INK4a}$ protein (Fig. 3a, b). Gene expression analysis showed up-regulation of *PDGFRA* and *RB*1, and down-regulation of *CDKN2A* genes relative to normal tissues (Fig. 3c). *RB*1 was overexpressed compared to other grades of astrocytoma.

### Copy number analysis

Copy number analysis of Affymetrix SNP Array 6.0 data from SF7761 DNA revealed three large and 23 small regions of copy number alteration (CNA, Table 1; Fig. 4). The large CNAs include an extra copy of the q arm of chromosome 1, whole chromosome 2, and most of the q arm of chromosome 3. The small regions include 18 regions of hemizygous deletion, 3 regions of single copy gain, and 2 regions of homozygous deletion. Five of the small CNA regions were frequently observed in TCGA

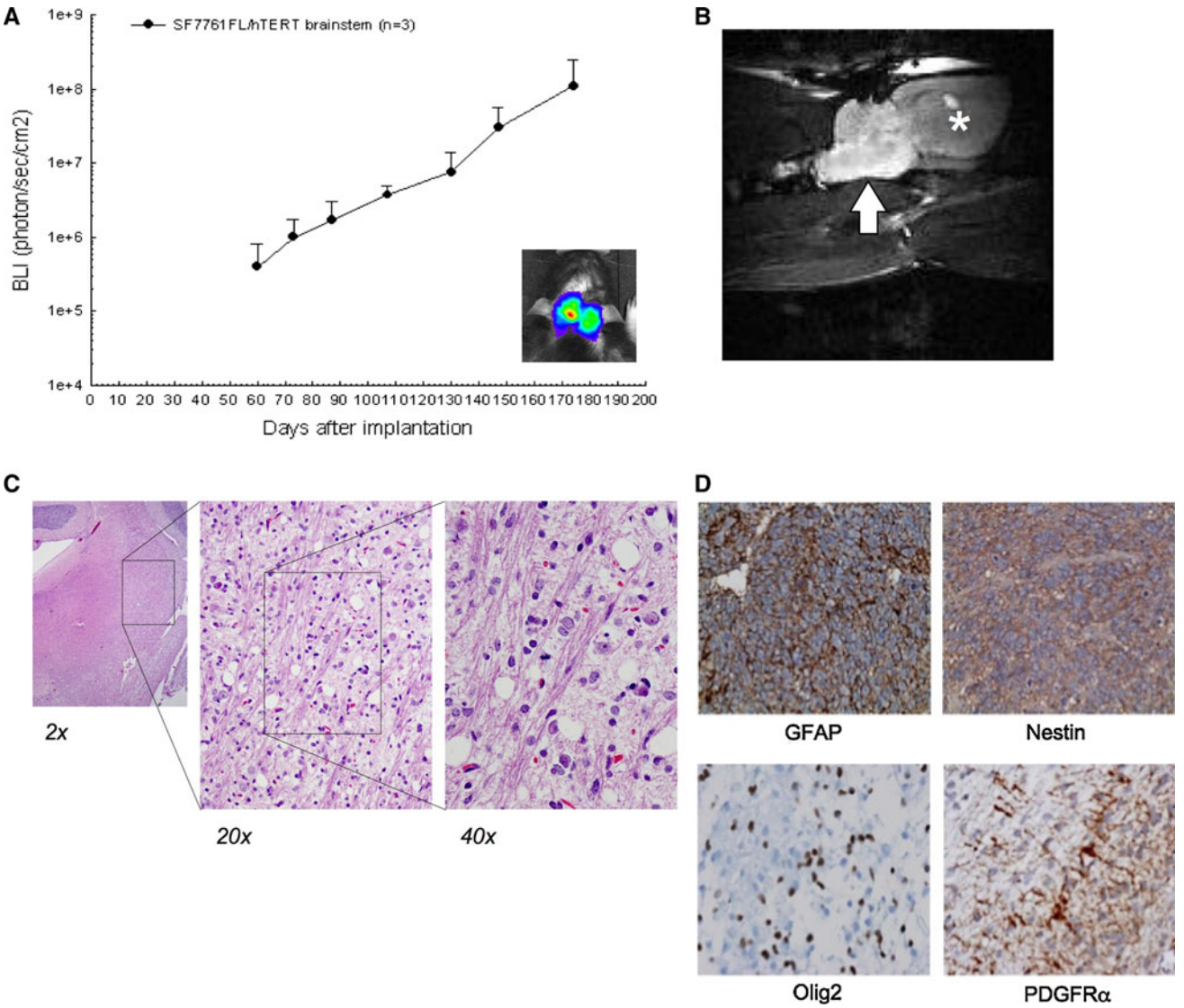


**Fig. 2** Association between bioluminescence signal and corresponding tumor volume in rats receiving brainstem injection of SF7761 cells. **a** Implantation of tumor cells in the rodent pons is detectable with BLI. **b** MR imaging shows high signal within the pons (*arrow*), similar to the human imaging study. (The cerebral hemispheres are indicated by the *asterix*). **c** The histopathology shows a diffusely infiltrating tumor occupying the pons; once again similar to the human tissue sample. **d** Immunohistochemistry demonstrates that the tumor cells are positive for GFAP, Nestin, Olig2 (*scattered*), and PDGFRα

blood samples, so we presumed they are not specific to the SF7761 cell line. In association with this summary, it is noteworthy that copy number deviations responsible for the most common gene alterations in adult malignant glioma, such as PTEN, CDKNA, and TP53 deletion, and EGFR amplification, were not found in SF7761 cells, suggestive of a distinct genetic etiology for DIPGs.

## Discussion

In this study we describe the establishment and initial characterization of a primary cell line derived from a human DIPG. The patient who underwent biopsy presented with typical symptoms prior to diagnosis, and her MRI scan was consistent with a diffusely infiltrative tumor in the pons. At the time of initial imaging, the tumor did not have any features to suggest areas of malignant transformation (e.g. enhancement, or necrosis). Therefore, the surgical biopsy was obtained from a region of the tumor designed to minimize surgical complications and reduce the amount of brain tissue traversed by the biopsy needle. Although the clinical progression of this patient was completely consistent with a typical DIPG, with death occurring within a year, the pathological diagnosis of the tumor was a low grade (WHO grade II) astrocytoma. This discrepancy

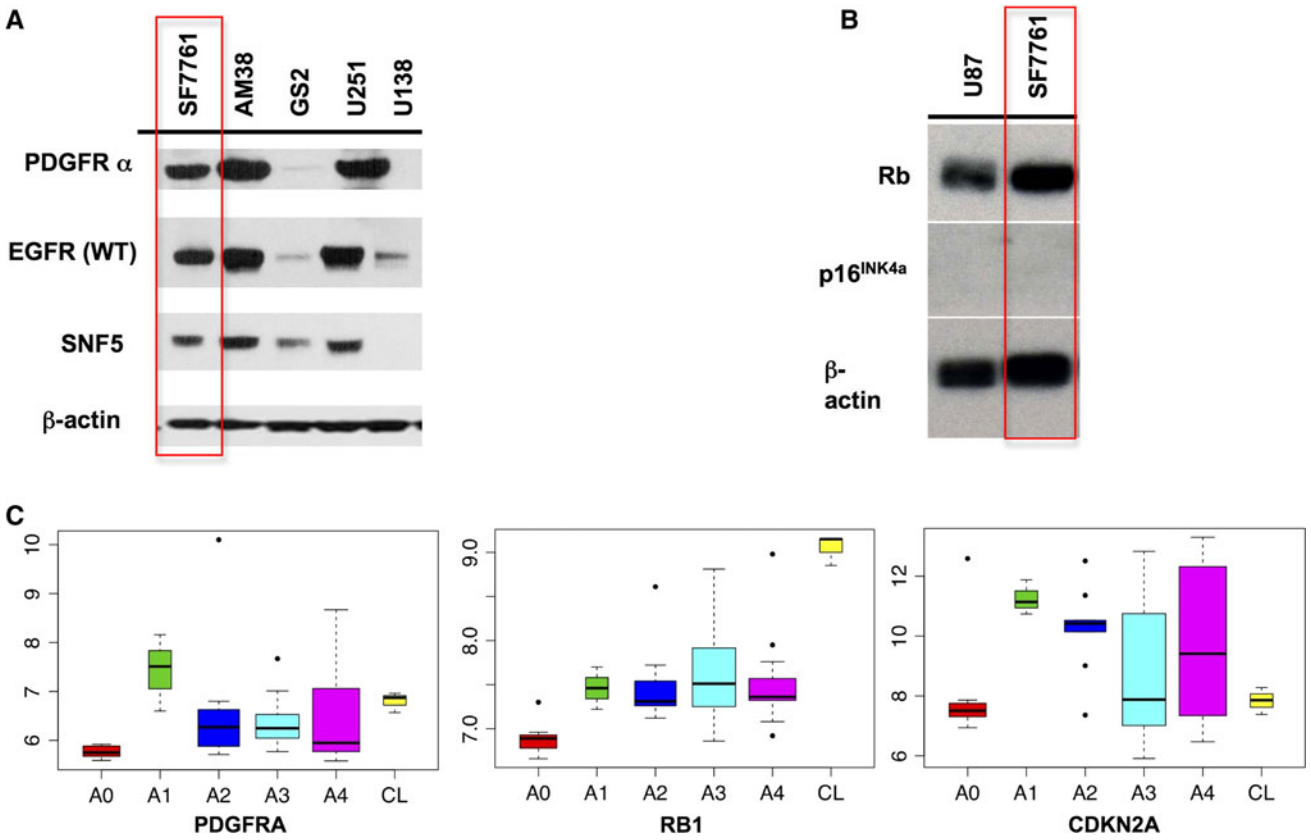


**Fig. 3** Protein and gene expression. **a**, **b** SF7761 demonstrates increased expression of PDGFRα, EGFR, SNF5, and Rb proteins, but reduced expression of $p16^{ink4a}$ protein. Expression of these proteins in the established cell lines AM38, GS2, U251, U138, and U87; all of which were originally derived from adult malignant gliomas, is shown for comparison. **c** Box plots expression of *PDGFRα*, *RB*1 and *CDKN2A* genes relative to normal tissue (*A0*), and supratentorial pediatric astrocytomas of varying grades (*A1–A4*) genes shows similarities to higher grade tumors, with the exception of *RB*1 which is expressed to a much higher degree. The y-axis represents $\log^2$ of quantile-normalized foreground signal

between the histopathology and the clinical outcome can be explained by the presence of tumor heterogeneity and the inherent sampling error that occurs when a small portion of the tumor is removed by biopsy.

Since the tissue specimen obtained for in vitro propagation was obtained from the same anatomic location as that for diagnostic purposes, it is not surprising that the explanted cells (presumably low grade in nature) did not demonstrate sustainable growth. Because of our prior experience in developing explant cultures from pediatric brain tumors, we prepared for the possibility of cell senescence by transducing these primary DIPG cells with hTERT retrovirus, in order to immortalize the cells and insure their sustainable propagation. This approach was successful in sustaining SF7761 in vitro growth, and for expanding SF7761 to an extent needed for in vivo experimentation. The in vivo growth rate of SF7761 cells is consistent with a slower growing tumor, and a pattern of infiltrative growth remarkably similar to what is observed in clinical specimens.

Sustainable tumorigenicity of SF7761 was demonstrated by passaging the tumor from primary culture to the brainstem, and then directly passaging the brainstem tumor from a symptomatic animal to a second generation animal host. Propagating the tumor in this manner also preserved its biological characteristics. Although rats are more accommodating for anatomic modeling and imaging is of brainstem xenografts, we have also successfully established SF7761 xenografts in the brainstem of athymic mice (data not shown), the use of which will help reduce costs of preclinical therapeutic testing.

Recent papers have demonstrated that there are unique alterations in pediatric gliomas as compared to their adult counterparts [17]. Not surprisingly, there may be regional differences between tumors that arise in the hindbrain as compared to the cerebral hemispheres, such as has been described for ependymomas arising in different CNS locations [18]. The copy number alterations in SF7761 (Table 1), in particular large gains in 1q and 2p, are similar to those reported in other studies [17]. Until very recently, none of the signaling pathways involved in DIPG formation were known. Two recent studies of pediatric high-grade gliomas noted that *PDGFRA* amplification occurred

**Table 1** Locations of genomic alterations and associated candidate gene involvement

| CNV call | Location (HG 18) | Length (kb) | Candidate genes |
|---|---|---|---|
| Loss | chr1:57013651–57066089 | 52 | BC048114, C1orf168, DKFZp686O04253 |
| Gain | chr1:143049286–247191011 | 104,142 | |
| Loss[a] | chr1:150819085-150853218 | 34 | LCE3B, LCE3C, LCE3D |
| Gain | chr2:2784–242738129 | 242,735 | |
| Loss[a] | chr2:34554898–34596540 | 42 | |
| Hdel[a] | chr2:52607972–52635046 | 27 | |
| Loss | chr3:8496450–8579079 | 83 | BC020876, LMCD1 |
| Loss | chr3:25195916–25373195 | 177 | |
| Loss | chr3:68611117–68647880 | 37 | FAM19A1 |
| Loss | chr3:74537938–74609897 | 72 | CNTN3 |
| Gain | chr3:130048665–199380515 | 69,332 | |
| Loss | chr4:15622146–15650717 | 29 | PROM1 |
| Loss | chr4:20012159–20260605 | 248 | SLIT2 |
| Loss | chr5:159911895–160094934 | 183 | ATP10B |
| Loss | chr7:103225594–103369042 | 143 | RELN |
| Hdel[a] | chr8:39354760–39506122 | 151 | ADAM5P, tMDC |
| Loss | chr8:122162372–122234914 | 73 | |
| Gain | chr8:130562330–130769277 | 207 | GSDMC |
| Gain | chr9:16893446–16982325 | 89 | |
| Loss | chr9:88447389–88482169 | 35 | |
| Loss[a] | chr12:9466943–9628505 | 162 | BX647938, CHLR1, DDX11 |
| Gain[a] | chr14:18611714–19505226 | 894 | A26C2, AK022914, AK056135, AY338952, AY338954, AY458019, BC016035, BC017398, BC040855, BC041856, BX248778, DQ583164, DQ583610, DQ590589, DQ591735, DQ595048, DQ595091, DQ786293, OR4K1, OR4K2, OR4K5, OR4M1, OR4N2, OR4Q3, POTEG |
| Loss | chr16:75651045–75716878 | 66 | |
| Loss | chr17:3522296–3594962 | 73 | GSG2, ITGAE, P2RX5, TAX1BP3, TMEM93 |
| Loss | chr17:41044105–41569943 | 526 | AX747136, BC018035, BC069230, CRHR1, IMP5, KIAA1267, MAPT, MGC57346, STH |
| Loss | chr22:16734350–16868132 | 134 | KIAA1364, MICAL3 |

[a] Area of frequent genomic CNAs and/or segmental duplication

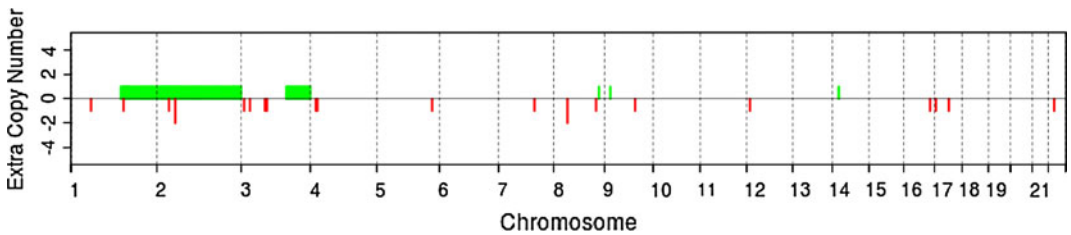


**Fig. 4** Chromosome copy number. SF7761 cells demonstrate gain of chromosomes 1q, 2, and 3q. Smaller regions of chromosome gain are also visible (*9*, *8*, and *11*). No large regions are deleted

in 29–36 % of DIPGs [17, 19]. Up-regulation of PDGFR signaling in Nestin$^{+}$ cells of the IVth ventricle subventricular zone [20], or cells of the dorsolateral pons [21] results in formation of glioblastoma in mouse models. Our analysis reveal that SF7761 cells have elevated PDGFRα and Rb, but lack expression of the tumor suppressor p16$^{INK4a}$ (Fig. 2). These cells also express Nestin and Olig2. Because of the very small size of the initial biopsy, we did not have remaining sections to confirm Nestin and Olig2 expression in the original tumor. A recent paper also

described the isolation and characterization of a DIPG-derived cell line from autopsy-derived tissue [12]. The patient in that study received three of a planned 30 fractions of radiation treatment before treatment was stopped. The characteristics of that cell line as grown in a rodent host were similar to SF7761 with diffuse infiltration of the brainstem. Neurospheres derived from that cell line were Nestin and GFAP positive with scattered positivity of Olig2; similar to our results (Fig. 2).

The limitations of this study include those that are associated with any model system that relies on human tumor growth in an immunodeficient animal. Although this model described in this study does not recapitulate the genetic alterations lead to de novo tumor formation, the phenotype of this xenograft tumor is strikingly similar to what is observed in the human disease. Another consideration is that hTERT modification of the primary cells will alter the growth features of the tumor. hTERT modification has been shown to increase the genomic instability of cells leading to additional copy number alterations [22]. In general, it is difficult to establish any permanent model system without an additional genetic modification.

There are two significant conclusions of this study. First, we demonstrate the feasibility of developing sustainable and tumorigenic DIPG cell sources that can be applied to therapeutic hypothesis testing. Typically, established cell lines derived from adult supratentorial gliomas are usually used as surrogates for many brain tumors, including DIPG. Cell lines such as SF7761 allows the use of a much more appropriate biological model. The development of such resources should also aid in addressing the extent of genetic variation between malignant DIPGs, which could prove important for DIPG subclassification and corresponding individualization of treatment for patients with this cancer.

Second, the particular pathologic features observed in this case sheds some light on the molecular pathogenesis of DIPGs. In general, relative to the extent of the brainstem that is infiltrated with tumor as shown by MR imaging, most patients usually present with mild or minor symptoms. The paucity of symptoms suggest that most DIPG tumors are present for a long time as a lower grade neoplasm that slowly infiltrates the pontine tegmentum. This is consistent with the WHO grade II histopathology of the tumor specimen that was obtained from this patient. The development of symptoms in most patients, however, probably coincides with the transformation of the pre-existing low grade tumor into a malignant genotype, which then leads to rapid neurologic decline and death. It is likely that this early transformation precedes the development of detectable MRI changes. This hypothesis could be addressed through analysis of tumor specimens over time, or a comparison of distinct tumor specimens obtained from the same patient.

Although this interpretation is speculative, it is possible that the genetic profile of DIPGs will demonstrate a stepwise series of genetic mutations, perhaps similar to infiltrative astrocytomas seen in the cerebral hemispheres in young adults. Identification of these genetic changes occurring early in oncogenesis will hopefully direct the selection of effective therapeutic agents. It is this objective that makes the characterization of tumor specimens early in the disease progression particularly important.

**Acknowledgments** This study was supported by the Pediatric Brain Tumor Foundation Institute Award to the University of California San Francisco, and Timmy's Rainbow Foundation for Brainstem Tumor Research. The authors also thank Dr. Susan Baker (St. Jude's Children's Hospital and Medical Center) for allowing permission to examine copy number data from a published data set of pediatric astrocytic tumors.

## References

1. Donaldson SS, Laningham F, Fisher PG (2006) Advances toward an understanding of brainstem gliomas. J Clin Oncol 24(8):1266–1272. doi:10.1200/JCO.2005.04.6599
2. Recinos PF, Sciubba DM, Jallo GI (2007) Brainstem tumors: where are we today? Pediatr Neurosurg 43(3):192–201. doi:10.1159/000098831
3. Finlay JL, Zacharoulis S (2005) The treatment of high grade gliomas and diffuse intrinsic pontine tumors of childhood and adolescence: a historical - and futuristic -perspective. J Neurooncol 75(3):253–266. doi:10.1007/s11060-005-6747-7
4. Sharp JR, Bouffet E, Stempak D, Gammon J, Stephens D, Johnston DL, Eisenstat D, Hukin J, Samson Y, Bartels U, Tabori U, Huang A, Baruchel S (2010) A multi-centre Canadian pilot study of metronomic temozolomide combined with radiotherapy for newly diagnosed paediatric brainstem glioma. Eur J Cancer 46(18):3271–3279. doi:10.1016/j.ejca.2010.06.115
5. Huse JT, Phillips HS, Brennan CW (2011) Molecular subclassification of diffuse gliomas: seeing order in the chaos. Glia 59(8):1190–1199. doi:10.1002/glia.21165
6. Phillips HS, Kharbanda S, Chen R, Forrest WF, Soriano RH, Wu TD, Misra A, Nigro JM, Colman H, Soroceanu L, Williams PM, Modrusan Z, Feuerstein BG, Aldape K (2006) Molecular subclasses of high-grade glioma predict prognosis, delineate a pattern of disease progression, and resemble stages in neurogenesis. Cancer Cell 9(3):157–173. doi:10.1016/j.ccr.2006.02.019
7. Paugh BS, Broniscer A, Qu C, Miller CP, Zhang J, Tatevossian RG, Olson JM, Geyer JR, Chi SN, da Silva NS, Onar-Thomas A, Baker JN, Gajjar A, Ellison DW, Baker SJ (2011) Genome-wide analyses identify recurrent amplifications of receptor tyrosine kinases and cell-cycle regulatory genes in diffuse intrinsic pontine glioma. J Clin Oncol 29(30):3999–4006. doi:10.1200/JCO.2011.35.5677
8. Wu G, Broniscer A, McEachron TA, Lu C, Paugh BS, Becksfort J, Qu C, Ding L, Huether R, Parker M, Zhang J, Gajjar A, Dyer MA, Mullighan CG, Gilbertson RJ, Mardis ER, Wilson RK, Downing JR, Ellison DW, Baker SJ (2012) Somatic histone H3 alterations in pediatric diffuse intrinsic pontine gliomas and non-brainstem glioblastomas. Nat Genet. doi:10.1038/ng.1102
9. Aoki Y, Hashizume R, Ozawa T, Banerjee A, Prados M, James CD, Gupta N (2012) An experimental xenograft mouse model of diffuse pontine glioma designed for therapeutic testing. J Neurooncol. doi:10.1007/s11060-011-0796-x

10. Hashizume R, Ozawa T, Dinca EB, Banerjee A, Prados MD, James CD, Gupta N (2010) A human brainstem glioma xenograft model enabled for bioluminescence imaging. J Neurooncol 96(2):151–159. doi:10.1007/s11060-009-9954-9
11. Caretti V, Zondervan I, Meijer DH, Idema S, Vos W, Hamans B, Bugiani M, Hulleman E, Wesseling P, Vandertop WP, Noske DP, Kaspers G, Molthoff CF, Wurdinger T (2010) Monitoring of tumor growth and post-irradiation recurrence in a diffuse intrinsic pontine glioma mouse model. Brain Pathol. doi:10.1111/j.1750-3639.2010.00468.x
12. Monje M, Mitra SS, Freret ME, Raveh TB, Kim J, Masek M, Attema JL, Li G, Haddix T, Edwards MS, Fisher PG, Weissman IL, Rowitch DH, Vogel H, Wong AJ, Beachy PA (2011) Hedgehog-responsive candidate cell of origin for diffuse intrinsic pontine glioma. Proc Natl Acad Sci U S A 108(11):4453–4458. doi:10.1073/pnas.1101657108
13. Sanai N, Wachhorst SP, Gupta NM, McDermott MW (2008) Transcerebellar stereotactic biopsy for lesions of the brainstem and peduncles under local anesthesia. Neurosurgery 63(3):460–466; discussion 466–468. doi:10.1227/01.NEU.0000324731.68843.74
14. Gunther HS, Schmidt NO, Phillips HS, Kemming D, Kharbanda S, Soriano R, Modrusan Z, Meissner H, Westphal M, Lamszus K (2008) Glioblastoma-derived stem cell-enriched cultures form distinct subgroups according to molecular and phenotypic criteria. Oncogene 27(20):2897–2909. doi:10.1038/sj.onc.1210949
15. Dinca EB, Sarkaria JN, Schroeder MA, Carlson BL, Voicu R, Gupta N, Berger MS, James CD (2007) Bioluminescence monitoring of intracranial glioblastoma xenograft: response to primary and salvage temozolomide therapy. J Neurosurg 107(3):610–616. doi:10.3171/JNS-07/09/0610
16. Wang K, Li M, Hadley D, Liu R, Glessner J, Grant SF, Hakonarson H, Bucan M (2007) PennCNV: an integrated hidden Markov model designed for high-resolution copy number variation detection in whole-genome SNP genotyping data. Genome Res 17(11):1665–1674. doi:10.1101/gr.6861907
17. Paugh BS, Qu C, Jones C, Liu Z, Adamowicz-Brice M, Zhang J, Bax DA, Coyle B, Barrow J, Hargrave D, Lowe J, Gajjar A, Zhao W, Broniscer A, Ellison DW, Grundy RG, Baker SJ (2010) Integrated molecular genetic profiling of pediatric high-grade gliomas reveals key differences with the adult disease. J Clin Oncol 28(18):3061–3068. doi:10.1200/JCO.2009.26.7252
18. Johnson RA, Wright KD, Poppleton H, Mohankumar KM, Finkelstein D, Pounds SB, Rand V, Leary SE, White E, Eden C, Hogg T, Northcott P, Mack S, Neale G, Wang YD, Coyle B, Atkinson J, DeWire M, Kranenburg TA, Gillespie Y, Allen JC, Merchant T, Boop FA, Sanford RA, Gajjar A, Ellison DW, Taylor MD, Grundy RG, Gilbertson RJ (2010) Cross-species genomics matches driver mutations and cell compartments to model ependymoma. Nature 466(7306):632–636. doi:10.1038/nature09173
19. Zarghooni M, Bartels U, Lee E, Buczkowicz P, Morrison A, Huang A, Bouffet E, Hawkins C (2010) Whole-genome profiling of pediatric diffuse intrinsic pontine gliomas highlights platelet-derived growth factor receptor alpha and poly (ADP-ribose) polymerase as potential therapeutic targets. J Clin Oncol 28(8):1337–1344. doi:10.1200/JCO.2009.25.5463
20. Becher OJ, Hambardzumyan D, Walker TR, Helmy K, Nazarian J, Albrecht S, Hiner RL, Gall S, Huse JT, Jabado N, MacDonald TJ, Holland EC (2010) Preclinical evaluation of radiation and perifosine in a genetically and histologically accurate model of brainstem glioma. Cancer Res 70(6):2548–2557. doi:10.1158/0008-5472.CAN-09-2503
21. Masui K, Suzuki SO, Torisu R, Goldman JE, Canoll P, Iwaki T (2010) Glial progenitors in the brainstem give rise to malignant gliomas by platelet-derived growth factor stimulation. Glia 58(9):1050–1065. doi:10.1002/glia.20986
22. Wen VW, Wu K, Baksh S, Hinshelwood RA, Lock RB, Clark SJ, Moore MA, Mackenzie KL (2006) Telomere-driven karyotypic complexity concurs with p16INK4a inactivation in TP53-competent immortal endothelial cells. Cancer Res 66(22):10691–10700. doi:10.1158/0008-5472.CAN-06-0979